Accepted Manuscript

Predictions of the maximum energy extracted from salinity exchange inside porous electrodes
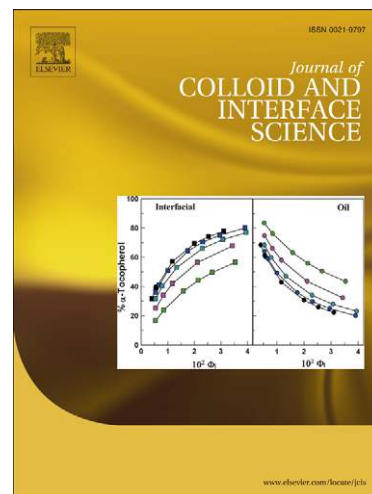
M.L. Jiménez, M.M. Fernández, S. Ahualli, G. Iglesias, A.V. Delgado

Predictions of the maximum energy extracted from salinity exchange inside porous electrodes

M.L. Jiménez*, M.M. Fernández, S. Ahualli, G. Iglesias, A.V. Delgado

Department of Applied Physics, School of Sciences, University of Granada, 18071, Granada, Spain.

Abstract

Capacitive energy extraction based on double layer expansion (CDLE) is the name of a new method devised for extracting energy from the exchange of fresh and salty water in porous electrodes. It is based on the change of the capacitance of electrical double layers (EDLs) at the electrode/solution interface when the concentration of the bulk electrolyte solution is modified. The use of porous electrodes provides huge amounts of surface area, but given the typically small pore size, the curvature of the interface and EDL overlap should affect the final result. This is the first aspect dealt with in this contribution: we envisage the electrode as a swarm of spherical particles, and from the knowledge of their EDL structure, we evaluate the stored charge, the differential capacitance and the extracted energy per CDLE cycle. In all cases, different pore radii and particle sizes and possible EDL overlap are taken into account. The second aspect is the consideration of finite ion size instead of the usual point-like ion model: given the size of the pores and the relatively high potentials that can be applied to the electrode, excluded volume effects can have a significant role. We find an extremely strong effect: the double layer capacitance is maximum for a certain value of the surface potential. This is a consequence of the limited ionic concentration at the particle-solution interface imposed by the finite size of ions, and leads to the presence of two potential ranges: for low electric potentials the capacitance increases with the ionic strength, while for large potentials we find the opposite trend. The consequences of these facts on the possibility of net energy extraction from porous electrodes, upon changing the solution in contact with them, are evaluated.

Keywords: CapMix, Electric double layer expansion, Energy extraction from salinity exchange, Ionic size effects

*Corresponding Author
 Email address:* `jimenezo@ugr.es` (M.L. Jiménez)

1. Introduction

The search for renewable energy sources is a non-stop race against the irreversible damage of our planet. Although wind and solar energies are leading such race, interestingly enough colloid scientists have in their hands tools that can contribute to some extent, not fully quantified yet, probably. Some methods are already available based on the behavior of interfaces under salinity changes: Wick and Schmitt [1] gave an account of the possibilities of gaining energy in sea environments. The fundamentals of the methods are related to the free energy release achieved by mixing solutions of different ionic strengths; in the particular case of sea and fresh water (roughly 600 mM and 20 mM respective ionic strengths), mixing 1 L of river water with large amounts of sea water would produce 2 kJ [2, 3]. As a whole, if all this energy could be extracted throughout the world coasts, 2 TW of power could be made available, that is, roughly the total world electricity demand [1, 4].

Research must hence be focussed on the implementation of methods through which that huge amount of energy, or at least a significant part of it, can be effectively extracted. Desalination techniques operated in reverse are good candidates, in particular, pressure-retarded osmosis (PRO) [1, 5, 6], and reverse electrodyalisis (RED) [4, 7]. In the former, fresh water is allowed to flow through a semipermeable membrane into a pressurized sea water chamber; this high-pressure solution is used to obtain electrical energy by depressurizing it through a turbine. In RED, concentrated salt solutions and fresh water flow through alternating cells which are separated by ion exchange membranes; the cells will be alternatively enriched in cations and anions, thus producing, respectively, negative and positive potentials at the corresponding electrodes. If the number of cells connected is large enough, the total voltage will be larger than the electrode reaction potential, and energy can be extracted. Although considerable advances have been produced in both techniques [8, 9, 10, 11, 12, 13], they are mostly at the laboratory scale. In addition, they present clear drawbacks which must be dealt with, concerning mainly membrane selectivity, fouling and cost, and the necessity of using additional converters such as turbines for effectively producing electricity.

This gives an opportunity to alternative technologies, for instance, the one that will be considered in this article, which was first suggested by Brogioli [14], and extended to lab-scale experiments by Brogioli et al [15]. This method is enclosed in a group of emergent technologies jointly known as *Capmix* methods [16], which are based on the change of the electrical properties of the electrode-solution interface associated to salinity variations. Their aim is to directly extract electric energy without conversions through turbines and thermal machines. Capmix encloses two groups of techniques, one (capacitive energy extraction by Donnan potential or CDP, [17, 18, 19, 20, 21]) uses ion-selective membranes adjacent to the porous electrodes, so that, during the generation of the Donnan potentials in the respective membranes (one anionic and the other cationic), electric current flows in the external circuit [17]. The process can proceed continuously, so that when the ionic concentration in the cell is

2

modified (for instance, exchanging sea and river waters) electrons flow externally from one electrode to the other and ions flow inside the cell. It is worth mentioning that the technique reciprocal of CDP is deionization by the use of ultra-capacitors [22]. Subsequent works dealing with this technique focused on improving the power output and lowering the ohmic losses [21], which is one of the major issues in all electrochemical techniques. In these respect, recent works have revealed that the use of wire-shaped instead of flat plate electrodes means a very significant improvement in both issues mentioned. In addition, such a design provides a faster time response, and hence, higher power output [22, 20].

The second group of techniques, known as capacitive energy extraction based on double layer expansion (CDLE, [14, 15, 23, 24, 25, 26]), is based on the fact that electrical double layers (EDLs) can accumulate a large amount of charge if the interfacial area is high enough, and that the capacitance of the EDL depends very significantly on the ionic contents of the medium [25]. If a metal/solution interface is externally charged (using a battery, for instance) in the presence of high ionic strength, and discharged in low ionic strength (less capacitance, more potential for given charge), it might be possible to obtain a net amount of energy: the electrodes are charged at our expense in conditions of lower voltage, and discharged (delivering power) at higher voltage. The result is that electrical work is made available, without use of any kind of selective membranes or electromechanical converters, like dynamos or turbines [14, 15, 24].

In order to increase the charge transfer, electrodes made of microporous carbon particles can be used because of their huge surface area. However, since the charging potential can be relatively high (several hundred mV) and the pore diameter can be as low as 1 nm, simple models assuming low potentials and planar interfaces may not describe accurately the phenomenon. Furthermore, the behavior of the ions close to the wall is another source of difficulty, as they can even lose their hydration shell (fully or in part) under the EDL field. This is the case of ionic liquids [27, 28], and is the basis of the supercapacitances that are found with activated carbons with pores of size below 1 nm, but can happen even for small, monovalent, well hydrated ions like Na^+, as has been shown by molecular dynamics simulation [29]. As a consequence, a Stern layer can be formed with ions located between the inner and outer Helmholtz planes, which are partially dehydrated due to strong chemical or electric interactions with the surface. However, there is no evidence of such strongly adsorbed ions at the carbon-sodium chloride interface, and in our model the traditional image of a charge-free Stern layer determined by the distance of minimum approach of hydrated Na^+ and Cl^- ions will be considered.

We will focus on the modeling of the solution-pore wall interface inside the porous material, which is of course just part of the description of the complete electrode. This is far more complex than we can reach in this contribution. As in other analyses of the electrochemistry of porous electrodes, time effects will be ignored and only steady state situations will be considered (a model including a kinetic analysis of the electrode response has been described recently by Rica et al. [24, 26]); furthermore, no distinction will be made on the exact position in the electrode of the interface being described, an issue that is of

3

utmost importance when modeling the whole electrode, as discussed by New-man and Tobias [30]. These authors stressed that the macroscopic description means in fact an average of the variables of interest over regions small in comparison with the whole electrode but large in relation to the typical pore size. Computational simulations, on the contrary, require some assumption regarding the pore geometry. For instance, Lim et al. [31] considered cylindrical pores with semicircular openings, whereas Yamada et al. [32] based their model on a swarm of spherical porous particles, very much like one of the proposals of the present contribution. Considerable effort has been reported on the modeling of the electrodes in terms of transmission lines with distributed capacitance and resistance [33, 34, 35]. This approach has been extended to consider networks going from macro- to micro-pores, as in [36, 37].

For our purposes, existing models on the description of the EDL potential profile at interfaces with different geometries [38, 34, 39, 40, 41, 42, 43, 44, 45] cannot be applied to porous electrodes because such models are usually restricted to dilute suspensions, so that the likely overlap between EDLs from opposite walls of the pores is not considered. Theoretical models including EDL overlap and ionic size effects have been applied to salt free suspensions [42], and are based on cell models, which are appropriate in the case of homogeneous distributions of non-contacting spherical particles [41].

In this work, we propose an approach in which the porous electrodes are modelled as a swarm of spherical particles. We will include the following aspects in our simulations:

- Non-Planar EDL: inside the activated particles, the most abundant pores are typically less than 10 nm in diameter, and curvature effects on the electric potential profile can be significant.

- EDL overlap: it is likely in the smallest pores and with the less concentrated solutions, considering that the potentials used for charging can be relatively high.

- Moderate charging potentials: larger energies can in principle be obtained if large amounts of charge are transferred back and forth at very different potentials. For fixed values of the salinity, it may be necessary to explore potential differences as high as 500-600 mV. In such conditions, the interfacial region can be largely enriched in counterions, to the extent that the point charge hypothesis for EDL structure leads to unrealistically high counterion concentrations in the vicinity of the pore wall. This fact, together with the high salinity of the sea water, means a non-negligible role of the size of the ions.

Such treatment will lead to a theoretical prediction of the maximum energy that can be physically extracted in a CDLE technique. In this model, design-dependent issues, such as ohmic losses, pumping energy requirements, ineffective wetting and others are not considered. Nevertheless, some predictions will be compared to experimental data on energy per CDLE cycle obtained with activated carbon particles.

4

2. Theoretical model

2.1. Principles of the technique

Fig. 1a is a schematic representation of the required setup. A couple of porous electrodes with high surface area (activated carbon, typically used in supercapacitors, is a good possibility, as shown in Fig. 1b) and assumed ideally polarizable, are wet with sea water [14]. The electrodes are, in the first step, connected to a battery, a potentiostat, or a supercapacitor set at a voltage below 1 V, in order to avoid the electrolytic decomposition of the solvent, and hence the appearance of Faradaic reactions [46], which will not be considered. The balance between diffusion and electrostatic interaction of both counterions and coions on each electrode will bring about the appearance of electric double layers and hence a profile of electric potential in the vicinity of the electrode (Fig. 2a). If sea water is exchanged for fresh water as the case may be in a river mouth, the potential profile would be different, as shown in Fig. 2b, where it is assumed that the exchange takes place in open circuit conditions. In that case, the surface charge density at the wall, σ, does not change and neither does the total charge at the EDL, which is redistributed in a thicker space. It can be seen that the electric potential increases (Fig. 2b). This is the key point in explaining the energy gain: if the CDLE cell, wetted with fresh water as mentioned, is connected to the external power source used for charging it, charge will flow from the cell to the external device until the cell potential equals that of the external source. Because the same amount of charge Q is given to the cell at some average potential V, and returned from the cell at a larger average potential $V + \Delta V$, a net energy $Q\Delta V$ is gained in each cycle.

Fig. 3 is a schematic representation of the energy extraction procedure [14]. The successive states of the system are as follows. A: electrodes in salt water connected to the battery at an initial potential Ψ_0; A→B: exchange for fresh water in open circuit (constant surface charge density σ_{AB}); B→C: battery reconnected in fresh water; C→D: exchange for salt water in open circuit (constant surface charge density σ_{CD}); D→A: battery reconnected in salt water. The area of the cycle represents the net extracted work per unit area of electrode. Hence, it is critical to properly calculate the relation between charge and potential at the EDL, in order to predict the experimental conditions leading to the maximum performance of the process. Parameters such as surface curvature, pore and ionic size affect such relation and they are the issue of this paper.

2.2. Point-like vs. finite-volume ions

Here we perform a mean field analysis of the structure of the EDL, and so, the electric potential distribution will be given by the Poisson equation:

$$\nabla^2 \Psi(\mathbf{r}) = -\frac{e\left(z^+ c^+(\mathbf{r}) + z^- c^-(\mathbf{r})\right)}{\varepsilon_0 \varepsilon_m} \tag{1}$$

In this equation, Ψ is the electrostatic potential at position $\mathbf{r}$, e the electron charge, $z^+(z^-)$ and $c^+(c^-)$ are the valences and number concentrations of
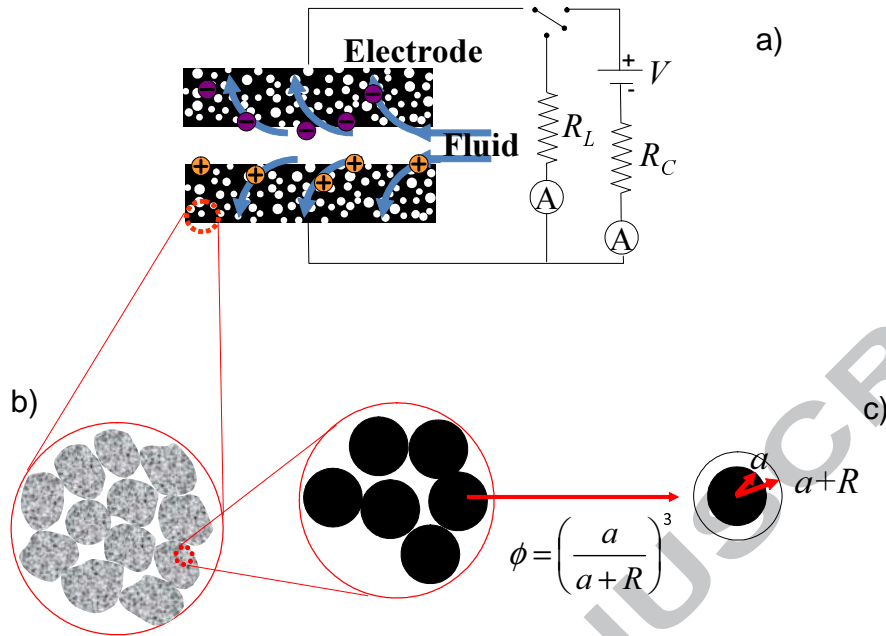
5

Figure 1: a) Schematic representation of the capacitive mixing cell; V is the charging voltage, and R_C, R_L are the resistors used for charging and discharging as external load, respectively; b) detail of the electrode; c) scheme of the cell model.

cations (anions) and ε_0 and ε_m are the electric permittivity of vacuum and the relative electric permittivity of the solvent, respectively.

In this work, this equation is first solved together with the Boltzmann distribution:

$$c^{\pm} = c_0^{\pm} \exp\left[-\frac{z^{\pm}e\Psi}{k_B T}\right] \qquad (2)$$

being $c_0^+(c_0^-)$ the bulk concentration of cations (anions) far from the particle surface, k_B the Boltzmann constant and T the absolute temperature. The model based on the Boltzmann distribution will be referred to as PIM (point ion model) hereafter.

Typical electrodes are made of a swarm of porous microparticles such that two kinds of pores are present: macropores (space between microparticles) and micropores (inside the microparticles themselves) as can be seen in Fig. 1b. The surface area associated to the latter is far larger than that of the former. For this reason, the whole electrode will be modelled as a concentrated suspension of spherical nanoparticles (Fig. 1c). The potential profile inside the pores will be hence represented by the potential around a given nanoparticle.

The most detailed analysis to date of the kinetics of ion transport and adsorption in the CDLE cell has been reported by Rica et al. [24, 26]. Based on a so-called 1D model of the transport of ions inside porous electrodes, elaborated
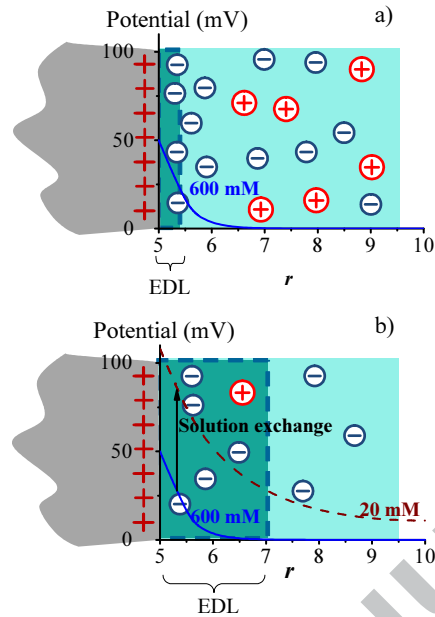
6

Figure 2: a) Electric potential profile in the vicinity of a spherical particle ($a = 5$ nm) in a cell of $a + R = 10$ nm, for a surface potential $\Psi_S = 50$ mV, and 600 mM NaCl solution; b) expected potential jump after exchanging the 600 mM solution for a 20 mM one at constant charge. The EDL limits in each case are marked by vertical dashed lines.

by Biesheuvel and Bazant [47], these authors combine a modified Donnan description of the diffuse EDL together with a charge-free Stern layer (to consider the limited approach of ions to the surface) as a description of the voltage drop at the carbon-solution interface inside the micropores. The main assumption of the modified Donnan approach is that the diffuse layer potential inside the micropores is constant, and it is controlled, for a given surface charge density on the wall, by the concentration of ions in the macropores of the electrode matrix. Such concentration in turn depends on the external bulk concentration through diffusion along a stagnant layer adjacent to the electrode, that is, the region where ion concentration changes from its bulk value to that at the carbon-solution interface. Consideration of diffusion of neutral salt and electrodiffusion of ions allows a very precise description of the time evolution of the CDLE cell potential in the different steps of the working cycle. In the present contribution we focus on the development of an accurate description of the structure and charge-potential relationships in the EDL of the micropores, without assuming planar geometry or constant wall potential. The kinetic aspects of the cycle as described in [24, 26] could be very useful, in connection with our model, to reach a complete and rigorous explanation of the CDLE technique.

The problem can be solved using a cell model (Fig. 1c), in which the whole system is substituted by a cell formed by a single particle whose radius a is
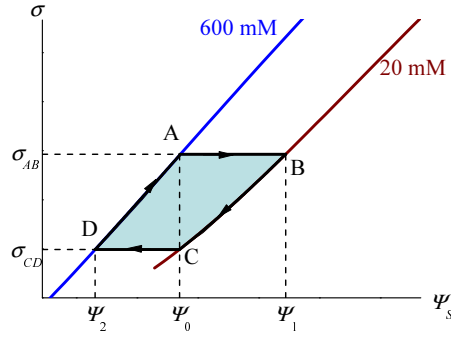
7

Figure 3: Schematic representation of the surface charge density vs. surface potential for two NaCl concentrations. A possible CDLE cycle is marked by arrowed lines. The area of the blue-shadowed region represents the energy extracted.

comparable to the thickness of the pore wall, surrounded by a shell of electrolyte, with thickness R, which will be identified with the pore radius. In this way, the particle size characterizes the tortuosity of the pore, while the cell size $a + R$ is chosen so as to preserve the volume fraction ϕ of the real system $(a^3/(a + R)^3 = \phi)$. The presence of particles in close vicinity to the reference one is modelled by an appropriate boundary condition for Eq. 2 at the limit of the cell:

$$\frac{d\Psi}{dr}\bigg|_{\bar{r}=R} = 0 \tag{3}$$

where $\bar{r} = r - a$ is the distance to the particle surface. According to Gauss law, this condition ensures the electroneutrality of the whole cell; it may also happen that the electric potential (and not only its derivative) is zero on the cell limit. This would be true if the cell thickness is larger than that of the EDL. However, if the case is that the EDL thickness is comparable to R, then the condition given by Eq. 3 will also be fulfilled, but EDL overlap would be implicit in such situation. This is important because considering the large volume fraction of nanoparticles required to mimic the electrode, the interparticle distances will be short and overlapping of neighbor double layers is very likely. Additionally, on the particle surface we have:

$$\Psi(\bar{r} = 0) = \Psi_S \tag{4}$$

With these equations, the potential profile can be calculated as a function of the surface potential, the particle concentration, the pore size, and the ionic concentration. The surface charge density, σ, is [48]:

$$\sigma = -\varepsilon_0 \varepsilon_m \frac{d\Psi}{dr}\bigg|_{\bar{r}=0} \tag{5}$$

Once the surface charge has been calculated, the differential capacitance of the

8

EDL per unit area, C_d, is obtained as

$$C_d = \frac{\mathrm{d}\sigma}{\mathrm{d}\Psi_S} \tag{6}$$

Finally, the extracted work in every cycle such as that represented by the shadowed area in Fig. 3 is:

$$W_S = \int_{\sigma_{CD}}^{\sigma_{AB}} \left[\Psi_S(20 \text{ mM}) - \Psi_S(600 \text{ mM})\right]\mathrm{d}\sigma \tag{7}$$

For practical purposes, it is convenient to normalize the extracted work to the electrode apparent (macroscopic) area, instead of the total interfacial area, and this new average work, W_S', can be calculated as:

$$W_S' = W_S \frac{3a^2}{(a+R)^3}d \tag{8}$$

where d is the thickness of the carbon layer. For the same reason, it may be of interest to evaluate the energy extracted per unit mass of carbon. This new quantity will be denoted W_m, and it can be evaluated as follows:

$$W_m = W_S \frac{3}{\rho a} \tag{9}$$

where ρ is the carbon density.

The interaction between ions can be taken into account by using sophisticated models as those existing in literature [40, 49, 50]. These models consider both coulombic and excluded volume interactions between every pair of ions instead of using a mean field approximation. They provide a detailed profile of the electric potential and predict interesting effects like charge inversion [40]. However, we are not interested in the precise profile of the electric potential, but rather in the effect of the finite volume of ions on the total stored charge in the EDL. Hence, we use a mean field approximation in which excluded volume is taken into account in the excess electrochemical potential of every ionic species i:

$$\mu_i^{excess} = k_B T \ln f_i \tag{10}$$

by an activity coefficient f_i that accounts for the ion-ion interaction. This approach will be referred to as extended-volume model (EVM) hereafter. An extensive analysis of the different approximations is given in [34, 51] and some consequences on the differential capacitance of the EDL are studied in [52].

We use the approximation provided in [53, 54], that leads to:

$$c^{\pm} = \frac{c_0^{\pm} \exp\left[-\frac{z^{\pm}e\Psi}{k_B T}\right]}{1 + \sum_{i=+,-} \frac{c_0^i}{c_{MAX}^i}\left[\exp\left(-\frac{z^i e\Psi}{k_B T}\right)\right]} \tag{11}$$

where c_{MAX}^i denotes the maximum concentration allowed for the corresponding ionic species. If, in addition, the existence of an excluded volume between

9

particle surface and hydrated ions is taken into account, then Eq. 1 must be solved separately in three regions. In the first one, between the particle surface and the radius of the smallest ion, say ion 1, $c_1(r) = c_2(r) = 0$. In the second region, where the biggest ion, say ion 2, cannot stay, we can write $c_2(r) = 0$. For larger distances to the surface, Poisson's equation (Eq. 1) must be solved considering both ionic species given by Eq. 11 [41]. Accordingly, new boundary conditions must be used, namely, the continuity of the potential and of the normal component of the electric displacement at the boundary between every pair of regions:

$$\Psi(\bar{r} = r_1^-) = \Psi(\bar{r} = r_1^+) \tag{12}$$

$$\Psi(\bar{r} = r_2^-) = \Psi(\bar{r} = r_2^+) \tag{13}$$

$$\left.\frac{\mathrm{d}\Psi}{\mathrm{d}r}\right|_{\bar{r}=r_1^-} = \left.\frac{\mathrm{d}\Psi}{\mathrm{d}r}\right|_{\bar{r}=r_1^+} \tag{14}$$

$$\left.\frac{\mathrm{d}\Psi}{\mathrm{d}r}\right|_{\bar{r}=r_2^-} = \left.\frac{\mathrm{d}\Psi}{\mathrm{d}r}\right|_{\bar{r}=r_2^+} \tag{15}$$

Note that the existence of a minimum distance of approach of ions to the pore wall (with thickness controlled by the ion radius) determines a charge-free inner layer at the edge of the diffuse layer. This was first hypothesized by Stern and has become an essential component of the classical electrochemistry of EDLs [34, 55]. This *Stern layer* is often modelled by a constant capacitance C^i, which is responsible for a significant part of the voltage drop when the diffuse layer capacitance grows to very high values (high electrolyte concentrations). The first quantitative evaluation of C^i dates back to Grahame, who performed differential capacitance measurements at the mercury-sodium fluoride interface [38]. He found that the experimental results could be explained if the relative electric permittivity of the Stern layer ε_i is around 18, and other authors found that ε_i can be as low as $\varepsilon_m/10$. According to Bazant et al. [34], Grahame was again the first author to propose a field dependent permittivity, introducing a critical value E_s of the local field in the EDL, beyond which the so-called *dielectric saturation* takes place: if $E > E_s$ the permittivity would rapidly change from ε_m to ε_i. The results shown in [34] demonstrate that consideration of a reduced permittivity of the Stern layer modifies very significantly the calculations of EDL capacitance when the classical Poisson-Boltzmann theory (with a PIM approximation) is used even for surface potentials as low as 50 mV. On the contrary, if it is the modified Poisson-Boltzmann model that is used, the effects are only appreciable in the vicinity of 250 mV. Hence, there is some equivalence between increasing the ionic size and decreasing ε_i, and electric saturation can be of lower importance than other effects, such as counterion crowding. For this reason, and considering that our main aim is evaluating the role of finite ion size and EDL overlap on the energy extracted, we will assume that the permittivity of the Stern layer is the same as that of the bulk solution. Other authors working with porous electrode interfaces [31, 47], and also with general interfaces follow the same approach, and even primitive models considering ion-ion correlations [40, 56, 57] are based on such hypothesis.

10

Since we may be dealing with high surface potentials, coions will be practically absent inside the EDL, and hence, the charge, electric potential profiles, the surface charge and differential capacitance will be mainly determined by the characteristics of the counterion. For this work we have studied in detail the case of NaCl, with hydrated radii $r_{Na^+} = 0.36$ nm ($c_{max}^+ = 6.3$ M) and $r_{Cl^-} = 0.33$ nm($c_{max}^+ = 8.$ M). From these values the maximum concentrations were calculated assuming the maximum packing fraction of hard spheres.

In Fig. 4 we illustrate the relevance of the excluded volume correction for the electric potential and counterion concentration in the case of moderate surface potential (100 mV) and salt concentration (600 mM). Using PIM, it can be observed that the largest part of the potential decay occurs in the first nanometer. Such behavior is not realistic since, based on excluded volume arguments, the ionic concentration cannot exceed the specified values. This modifies the predicted profiles of potential and concentrations, and limits the validity of the Boltzmann approximation to, for example, 160 mV for a 20 mM solution or 70 mV for a 600 mM solution.
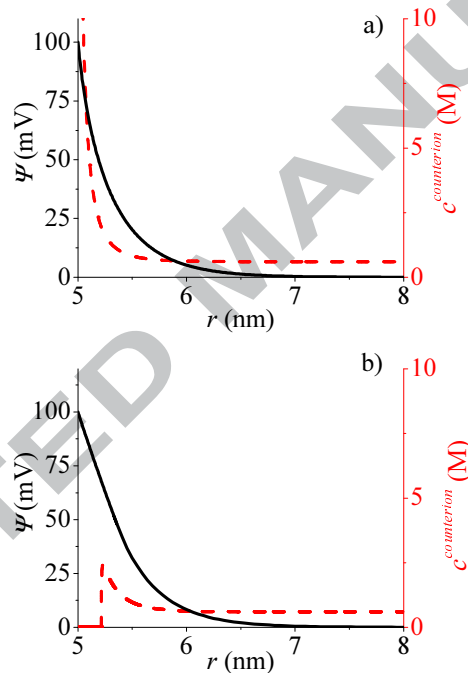

Figure 4: Potential (solid black line) and counterion concentration (dashed red line) profiles inside a pore for $\Psi_S = 100$ mV, $R = a = 5$ nm and $c = 600$ mM for model S. a) Point ion model. b) Finite volume ions with r(Na+) $= 0.36$ nm, r(Cl-) $= 0.33$ nm.

11

3. Experimental

3.1. Materials

The porous electrodes were kindly provided by Wetsus (The Netherlands). They are made of Norit DLC Super 30 activated carbon particles (Norit Nederland B.V., The Netherlands) deposited on a graphite current collector, using polyvinylidene fluoride (PVDF) as binder. The thickness of the carbon film is 250 μm. NaCl (from Scharlau, Germany) and deionized water (Milli-Q Academic, Millipore, France) were used in the preparation of the solutions.

3.2. Methods

The carbon films were cut into 9 mm radius disks and placed in contact with platinum collectors, by means of plastic or stainless steel rings, as shown in Fig. 5a,b. A pair of electrodes was inserted in a cylindrical glass cell, at the desired distance, and a microprocessor-controlled setup was used for switching on the pumps for filling the cells and opening the electrovalve for emptying it, as well as for establishing connection with the external power source (Bootscap cell supercapacitor, C = 350 F, Maxwell Technologies, USA) through the charging (R_C) or load (R_d) resistors (Fig.6). A Keithley 2700 (USA) multimeter provided with a data acquisition card was used for recording voltage and current at specified time intervals. In the charging stage, the electrodes, immersed in salty water (600 mM NaCl), were connected to the external supercapacitor previously charged at the desired voltage, through a 1 Ω resistor. After a given time (for this paper, we have chosen 1 min), and in open circuit conditions, the electrovalve is open, the 600 mM solution is discharged and the fresh water (20 mM) is pumped in. The voltage rise is subsequently recorded at 5 s intervals. In the examples shown (see below), the cell is connected again to the supercapacitor after the rise is completed, using $R_d = 70$ Ω. In this step, the charge initially given to the cell by the external capacitor is returned to it, although at a higher average voltage, due to the increase in the cell potential difference which has occurred after the fresh water entrance. Finally, the electrovalve is open again, the fresh water discarded and the salty solution is allowed in for starting a new cycle.

4. Results and discussion

4.1. Differential capacitance of the EDL

In Fig. 7a we summarize, the profiles of electric potential inside the pore as predicted by the EVM for the case of a 5 nm pore radius electrode immersed in NaCl solutions, with negative potential. Note that because the saturation in the counterion concentration extends over larger distances from the surface the larger $|\Psi_S|$, the average electrostatic interaction between the ions and the surface will be reduced if $|\Psi_S|$ is increased. This leads to a less efficient screening of the surface charge and hence, to flatter potential profiles and lower surface charge increase with surface potential, as compared to that attainable with point ions (Fig. 7b). In addition, due to excluded volume effects, increasing
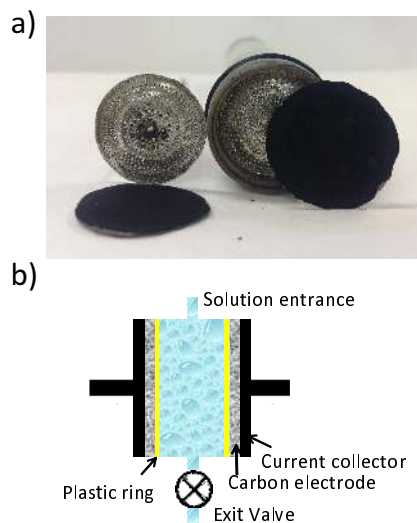
12

Figure 5: a) Electrodes used; b)Schematics of the CDLE cell.

the surface potential effectively means an increase in EDL thickness. Beyond a certain potential, such increase more than compensates for the surface charge density rise, and hence, the capacitance reaches a maximum (Fig. 7c), similar to the predictions of the Bikerman-Freise formula [34].

The significance of a finite volume consideration is made clear in Fig. 7b,c where the predictions of the PIM are included for the sake of comparison in the case of 20 mM NaCl. It can be seen that neglecting the actual ion dimensions may introduce important differences in the estimation of EDL quantities and mainly of the EDL capacitance and stored charge, even for low potentials, while for moderate to high charging potentials, such differences are of some orders of magnitude. Note that the capacitance maximum in Fig. 7c occurs at lower potentials as the ionic strength increases (around 400 mV for 1 mM and 150 mV for 600 mM): although the total accumulated charge is larger for larger ionic strengths, volume exclusion effects manifest themselves at lower potentials.

In the 600 mM case, an increase in surface potential (for example, from 200 mV to 400 mV), is mostly balanced by the excluded volume repulsion near the surface. Hence, ions accumulate far from the interface, as it would happen if the ionic strength were reduced. On the contrary, in the case of 20 mM, since excluded volume repulsion is not important, ions can accumulate close to the surface. As a consequence, at 600 mM the surface charge increases with potential more slowly than it does with 20 mM, leading to a lower EDL differential capacitance in the former case.

In Fig. 8a, b we compare the results obtained with different particle radii (solid lines). Let us first observe (Fig. 8a) that the charge stored at the surface decreases when the particle size raises, and in fact the values are increasingly
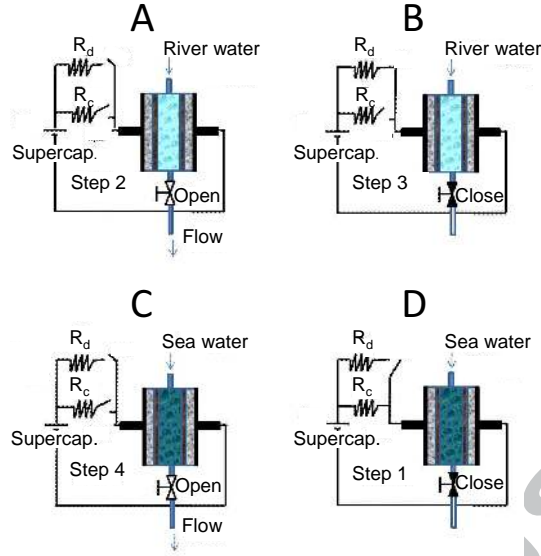
Figure 6: Circuit diagram for every step of the energy extraction cycle. Charging resistor, $R_C = 1\Omega$; load resistor, $R_d = 70\ \Omega$.

different from the PIM calculations. This suggests that the effect of ionic size is enhanced for larger particles in the electrode. In this case, the fraction of the EDL volume subtended by the unit area of surface is lower, that is, the volume available for the counterions is reduced. As a consequence, the effect of the excluded volume repulsion is magnified and the capacitance gets strongly reduced (Fig. 8b). Let us point out that for the conditions considered, these plots would have the same appearance for given radius and varying pore radii down to 2 nm, indicating that EDL overlap has little significance for the spherical geometry considered.

4.2. Extracted work

As mentioned, this investigation is justified by the possibility of obtaining a net amount of energy by properly taking advantage of the capacitance changes above described. In Fig. 9b we represent the amount of work W_S that can be obtained if one operating cycle as that drawn with arrows in Fig. 9a is performed. For the point ion model, W_S increases rapidly with the increase in potential, but, if the excluded-volume model is used instead, the capacitance cannot exceed a certain value, and as a consequence, neither can W_S. In fact, it is observed that this quantity reaches a maximum and smoothly decreases for larger potentials. This goes against the intuition, since one would expect larger stored charge and extracted work for increasing potentials, as also predicted by PIM. Viewed from another point, one can say that the energy depends on the distance between the curves $\sigma(\Psi_S)$ corresponding to low and high salt concentrations, and such
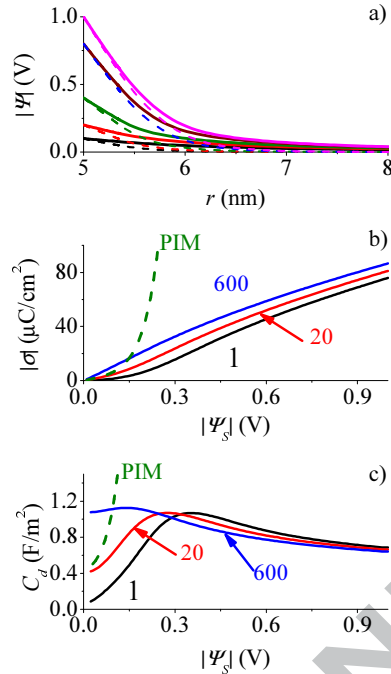
14

Figure 7: Electric potential profile (a) inside a pore of $R = a = 5$ nm, in 20 mM (solid lines) and 600 mM (dashed lines) NaCl solutions. The surface potentials correspond to the intercepts of the different curves, and range from 100 to 1000 mV. Surface charge density (b) and differential capacitance (c) as a function of surface potential for the same pore radius and the NaCl concentrations indicated (in mM). The green dashed lines in b) and c) are the point-ion model (PIM) predictions for 20 mM NaCl solution and 100 mV surface potential.

distance increases with the surface potential as long as the capacitance at 600 mM is larger than that at 20 mM. This occurs at low potentials (Fig. 7c), and hence W_S increases when the surface potential raises from zero to some critical value. At this point, the relation between the capacitances is reversed, so that when the capacitance in 600 mM solution falls below that in 20 mM, the $\sigma(\Psi_S)$ dependences approach each other, and the extracted energy declines even if we increase the charging voltage.

In Fig. 9b the tortuosity, determined by the particle radius, is fixed and the pore radius is increased. As we expected, the latter quantity has little effect on the extracted work. On the other hand, an important effect of the curvature of the pores is observed in Fig. 9c, where the pore radius is fixed and we vary the size a. Being the size of the pore the same in all cases, we can conclude that such decrease is a consequence of the finite ionic volume, as above mentioned.

The fact that the pore radius has little effect on the results of this model is in part a consequence of the studied ion/pore radius ratios. If the counterions present might have a larger effective size (for instance, in the case of multivalent counterions), it might happen that at a certain surface potential, the pore would
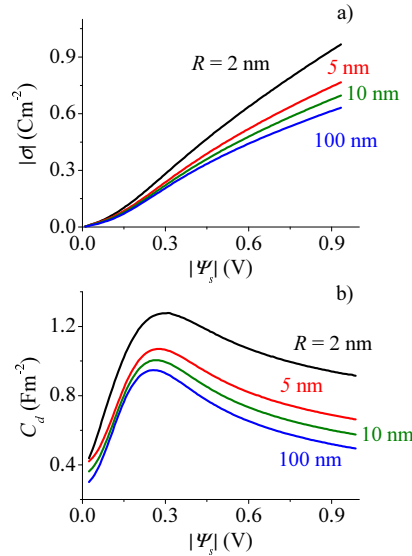
15

Figure 8: a) Surface charge density as a function of the surface potential for the pore radii indicated. b) Same as a) but for the differential capacitance.

get saturated with ions. In such a case, the potential decay would be slow and the charge at the pore surface might become independent of the surface potential. A CDLE cycle performed in these conditions would not produce a charge variation and the extracted work might eventually decay to zero.

At any rate, it will be clear that more energy can be harvested during operation if we increase the surface by decreasing either R or a. We have already mentioned that the surface-specific extracted work, W_S, increases upon decreasing a (Fig. 9c), but this effect is enhanced in W_m, as shown in Fig. 10a. Concerning the effect of the pore radius, although negligible on W_S (Fig. 9b) for the reasons already noted, it happens to be very significant when mass specific work is calculated (Fig. 10b), as a consequence of the associated increase in the interfacial area. This would represent, for a typical 1 mm electrode thickness the results illustrated in Fig. 10c,d.

It may be convenient, for comparison with other techniques, to have an estimation of the efficiency of the CDLE method. There is no definite way to do this, but one possibility is to compare the work obtained in one CDLE cycle with that achievable as proposed by Pattle [2]. Thus, the free energy decrease produced by the mixing of a volume of 20 mM solution equal to that in the pores of 1 g of electrode with a large volume of 600 mM (like in Pattle's estimation, [2] would be 7.18 J (for $R = a = 5$ nm). Comparing this value with the maximum energy extracted shown in Fig. 10b (charging voltage around 250 mV), the maximum efficiency would be 28%.
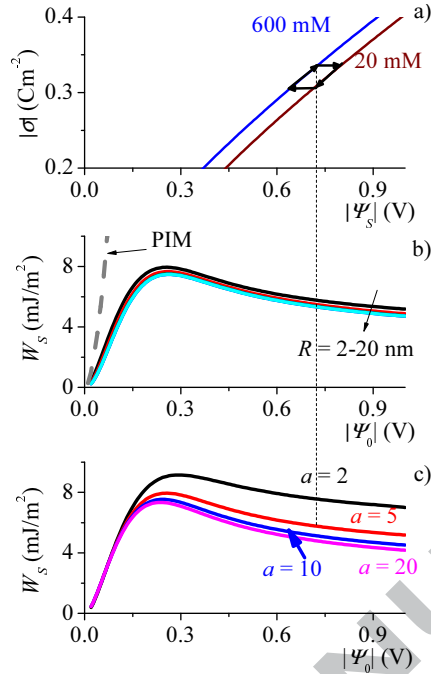
16

Figure 9: a) Surface charge density vs. surface potential for $a = R = 5$ nm and the NaCl concentrations indicated. One operation cycle is shown; b) specific extracted work for 20 mM-600 mM exchange, as a function of charging potential for $a = 5$ nm and different pore radii from 2 nm to 20 nm; c) specific extracted work as a function of charging potential for $R = 2$ nm and different particle radii in nm as indicated. The point ion model (PIM) predictions are shown in dashed grey for comparison.

4.3. Comparison with experimental data

Some of the theoretical results presented so far can be experimentally verified using the method above described. In particular, the expected voltage rise after exchanging salt and fresh water solutions is clearly observed in Fig. 11a, which illustrates the evolution of the voltage difference between both electrodes as a function of time when the filling solutions are interchanged. This is the required stage for extracting energy, and it is found that the energy extracted can be of the order of tens of mJ/m^2, relative to the apparent electrode area, as shown in Fig. 11c. We can see in this figure that increasing the charging voltage $2\Psi_0$ (below 1 V in all cases) produces a bell-shape dependence on the energy extracted per cycle, as a consequence of the behavior of the transferred charged depicted in Fig. 11b. As observed, for low values of the charging voltage Ψ_0, the energy increases with Ψ_0, a manifestation of the typical EDL behavior of increasing capacitance with ionic strength. On the contrary, beyond the maximum, ionic size effects limit the capacitance at 600 mM bringing it to values below the corresponding ones at 20 mM (Fig. 7) and decreasing the distance between the potentials at both ionic strengths. The same bell-shaped is observed
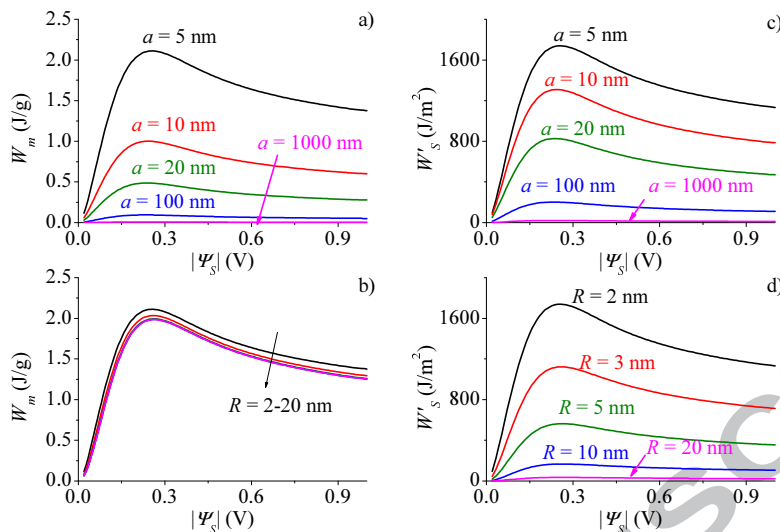
17

Figure 10: (a) Extracted work per unit mass of porous electrode for $R = 2$ nm and the a values indicated. b) The same but for $a = 5$ nm and the pore radius indicated. In all cases, $r^+ = 0.36$ nm and $r^- = 0.33$ nm. c) Same as a) but for the extracted work per unit apparent (macroscopic) area. d) Same as b) but for the extracted work per unit apparent area.

in the experimental evaluation of the transferred charge, this explaining the values of W_S' in Fig. 10c,d.

The qualitative agreement between data and predictions is clear, and even the charging potential for which the extracted energy is maximum agrees well with the predictions of our model. It must be noted, however, that the values of the extracted energy also depend on non measurable parameters in the experiment, such as the total surface area actually in contact with the solution, leakage, or the possibility of partial dehydration of counterions reducing their effective size. For these reasons, a quantitative agreement in Fig. 11c can only be reached if the wetted area is used as an adjustable parameter. However, the most relevant result is the confirmed existence of a maximum extracted work. Specifically, the decrease in extracted energy after the maximum is faster in our experiments than theoretically predicted. This is most likely a manifestation of the increased leakage when the charging potential is raised, an issue not considered in our model, but which can be found in electric circuit models like those elaborated in [35].

Experimental parameters are also determinant in evaluating the power available, since the time required to complete the cycle depends on the thickness of the electrode, and contact surface of the electrodes, the porosity of the carbon films, their hydrophobicity, and ultimately, on the optimization of the waiting time required to complete the voltage raise step. In our case, the typical duration of the cycle was, as mentioned, 9 min, and hence, the maximum power
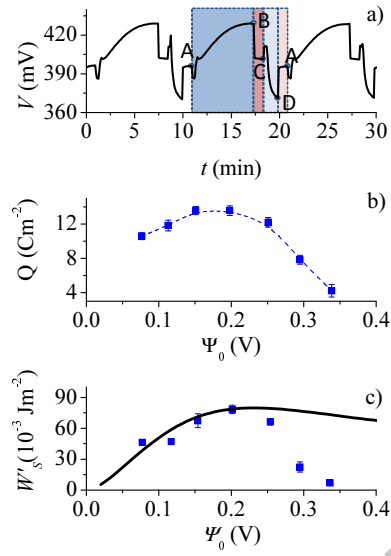
18

Figure 11: a) Examples of voltage evolution upon solution exchange. Symbols A, B, C and D correspond to those in Fig. 6c. b) Charge transferred during the discharge step (B in Fig. 6) for the indicated charging potentials. c) Energy extracted per cycle and unit area of apparent electrode surface. Symbols: experimental data for 250 μm electrode thickness. Solid line: theoretical predictions for pore radius $R = 2$ nm, particle size $a = 1000$ nm and 2% of wetted area. The dashed line is a guide for the eye. Error bars correspond to the standard deviation of the results obtained in at least 6 cycles.

would be around 0.13 mW/m^2, although this can be improved by decreasing the cycle duration and optimizing the carbon material selection [23, 24].

An additional concern about the use of carbon films for our energy extraction purposes would be the stability of the film after long term usage. In practical, large scale application, this could be faced by using a modular setup in which parts of the device could be replaced after aging without having to stop the whole process. In our case, one of the films was tested by continuous cycling during 8 days, and it was found that the overall decrease of the voltage raise was around 20%, which is probably about the limit acceptable for continuous operation.

The actual possibilities of the described technique in producing energy at useful scale must be confirmed by considering procedures to jump from the mW to at least the kW power ranges through proper design and association of smaller cells. It must be considered that the voltage rise is limited to tens of mV by the proper nature of the EDL, and this limit cannot be avoided. In particular, excluded volume effects in ions limit the total available work per cycle and prevent the use of the method for moderately high charging potentials.

It will be clear from the preceding discussions that mesoporous carbon elec-

19

trodes provide good conditions for a CDLE-based device, since they have a large interfacial area with low pore and particle radii. The possibilities of the CDLE technique remain open to further investigation. In the authors' opinion, the main topics to be considered in the near future include: *a)* Upscaling procedures; *b)* energy storage methods; *c)* implementation of detailed EDL models together with electrodiffusion analyses; *d)* evaluation of the role of the wetting characteristics of the carbon used and of its particular pore size distribution on the optimum CDLE performance; *e)* finally, consideration of aging and multi-ionic effects in the presence of actual or simulated sea water is also required to approach useful predictions of the CDLE results on real sites. Additionally, designers should also keep in mind that part of the energy produced will be unusable, considering that we may need to pump the solutions through the electrodes (or, at least, cyclically open and close ports to the solution reservoirs and valves for exit solutions), not to mention losses by spontaneous discharge of the storage supercapacitors, or internal resistance leakages in the CDLE cell itself.

5. Conclusions

We have presented a model for the extracted energy in an ideal cycle of the so-called capacitive energy extraction based on double layer expansion (CDLE). This model is based on the structure of the diffuse part of the EDL for a swarm of spherical particles tightly packed, and takes into account the possibility of EDL overlap and the finite size of the ions. We have analyzed the effects of the pore and particle sizes and the ionic strength, but the most significant results are observed when the ionic size is considered. We find that there is a surface potential delimiting two regions with different behaviors: for potentials lower than around 100 mV, the EDL qualitatively behaves as it does with point ion models, but at larger potentials, the ionic size limits the extracted energy that can be obtained with this method to far smaller values than those predicted for point ions. Also, in order to obtain the maximum energy, the electrode potential cannot exceed a value of around 250 mV and small particles and pores are desirable. Experimental data are presented, showing that the main prediction of our model, the existence of optimum charging potentials, is verified.

References

[1] G. L. Wick, W. R. Schmitt, Mar. Technol. Soc. J. 11 (1977) 16–21.

[2] R. E. Pattle, Nature 174 (1954) 660–660.

[3] R. S. Norman, Science 186 (1974) 350–352.

[4] J. N. Weinstein, F. B. Leitz, Science 191 (1976) 557–559.

[5] S. Loeb, Science 189 (1975) 654–655.

[6] A. Seppala, M. J. Lampinen, J. Membr. Sci. 161 (1999) 115–138.

[7] R. E. Lacey, Ocean Eng. 7 (1980) 1–47.

[8] J. W. Post, J. Veerman, H. V. M. Hamelers, G. J. W. Euverink, S. J. Metz, K. Nymeijer, C. J. N. Buisman, J. Membr. Sci. 288 (2007) 218–230.

[9] J. Veerman, M. Saakes, S. J. Metz, G. J. Harmsen, Chem. Eng. J. 166 (2011) 256–268.

[10] Y. Kim, B. E. Logan, Environ. Sci. Technol. 45 (2011) 5834–5839.

[11] P. Dlugolecki, A. Gambier, K. Nijmeijer, M. Wessling, Environ. Sci. Technol. 43 (2009) 6888–6894.

[12] T. Thorsen, T. Holt, J. Membr. Sci. 335 (2009) 103–110.

[13] K. Gerstandt, K. V. Peinemann, S. E. Skilhagen, T. Thorsen, T. Holt, Desalination 224 (2008) 64–70.

[14] D. Brogioli, Phys. Rev. Lett. 103 (2009) 058501.

[15] D. Brogioli, R. Zhao, P. M. Biesheuvel, Energy Environ. Sci. 4 (2011) 772–777.

[16] M. Bijmans, O. Burheim, M. Bryjak, A. Delgado, P. Hack, F. Mantegazza, S. Tenisson, H. Hamelers, Energy Procedia 20 (2012) 108 – 115.

[17] B. B. Sales, M. Saakes, J. W. Post, C. J. N. Buisman, P. M. Biesheuvel, H. V. M. Hamelers, Environ. Sci. Technol. 44 (2010) 5661–5665.

[18] B. B. Sales, F. Liu, O. Schaetzle, C. J. Buisman, H. V. Hamelers, Electrochimica Acta 86 (2012) 298 – 304.

[19] B. B. Sales, O. S. Burheim, F. Liu, O. Schaetzle, C. J. N. Buisman, H. V. M. Hamelers, Environ. Sci. Technol. 46 (2012) 12203–12208.

[20] O. S. Burheim, F. Liu, B. B. Sales, O. Schaetzle, C. J. N. Buisman, H. V. M. Hamelers, J. Phys. Chem. C 116 (2012) 19203–19210.

[21] F. Liu, O. Schaetzle, B. B. Sales, M. Saakes, C. J. N. Buisman, H. V. M. Hamelers, Environ. Sci. Technol. 5 (2012) 8642–8650.

[22] S. Porada, B. B. Sales, H. V. M. Hamelers, P. M. Biesheuvel, J. Phys. Chem. Lett. 3 (2012) 1613–1618.

[23] D. Brogioli, R. Ziano, R. A. Rica, D. Salerno, O. Kozynchenko, H. V. M. Hamelers, F. Mantegazza, Energy Environ. Sci. 5 (2012) 9870–9880.

[24] R. A. Rica, D. Brogioli, R. Ziano, D. Salerno, F. Mantegazza, J. Phys. Chem. C 116 (2012) 16934–16938.

[25] R. A. Rica, R. Ziano, D. Salerno, F. Mantegazza, D. Brogioli, Phys. Rev. Lett. 109 (2012) 156103.

[26] R. A. Rica, R. Ziano, D. Salerno, F. Mantegazza, M. Z. Bazant, D. Brogioli, Electrochimica Acta 92 (2013) 304 – 314.

[27] C. Merlet, B. Rotenberg, P. A. Madden, P.-L. Taberna, P. Simon, Y. Gogotsi, M. Salanne, Nat. Mater. 11 (2012) 306–310.

[28] M. Z. Bazant, B. D. Storey, A. A. Kornyshev, Phys. Rev. Lett. 106 (2011) 046102.

[29] A. Tanimura, A. Kovalenko, F. Hirata, Chem. Phys. Lett. 378 (2003) 638 – 646.

[30] J. S. Newman, C. W. Tobias, J. Electrochem. Soc. 109 (1962) 1183–1191.

[31] J. Lim, J. D. Whitcomb, J. G. Boyd, J. Varghese, Comput. Mech. 43 (2009) 461–475.

[32] Y. Yamada, T. Sasaki, N. Tatsuda, D. Weingarth, K. Yano, R. Kotz, Electrochim. Acta 81 (2012) 138–148.

[33] L. S. Shi, M. L. Crow, Proceedings of the General Meeting of the IEEE-Power-and-Energy-Society, Pittsburgh, PA (2008) 4691–4696.

[34] M. Z. Bazant, M. S. Kilic, B. D. Storey, A. Ajdari, Adv. Colloid Interface Sci. 152 (2009) 48–88.

[35] R. Faranda, Electric Power Systems Research 80 (2010) 363–371.

[36] M. Kaus, J. Kowal, D. U. Sauer, Electrochimica Acta 55 (2010) French Res Agcy.

[37] J. Kowal, E. Avaroglu, F. Chamekh, A. S'enfelds, T. Thien, D. Wijaya, D. U. Sauer, J. Power Sources 196 (2011) 573–579.

[38] R. Hunter, Foundations of Colloid Science, Oxford University Press, Oxford, 2000.

[39] S. Ahualli, M. L. Jiménez, F. Carrique, A. V. Delgado, Langmuir 25 (2009) 1986–1997.

[40] H. Greberg, R. Kjellander, J. Chem. Phys. 108 (1998) 2940–2953.

[41] J. J. López-García, M. J. Aranda-Rascón, C. Grosse, J. Horno, J. Phys. Chem. B 114 (2010) 7548–7556.

[42] R. Roa, F. Carrique, E. Ruiz-Reina, Phys. Chem. Chem. Phys. 13 (2011) 3960–3968.

[43] M. Plischke, D. Henderson, J. Chem. Phys. 88 (1988) 2712–2718.

[44] M. C. Henstridge, E. J. Dickinson, R. G. Compton, Chem. Phys. Lett. 485 (2010) 167 – 170.

[45] T. Goel, C. N. Patra, S. K. Ghosh, T. Mukherjee, J. Phys. Chem. B 115 (2011) 10903–10910.

[46] B. Conway, Electrochemical Supercapacitors: Scientific Fundamentals and Technological Applications, Kluwer Academic, New York, 1999.

[47] P. M. Biesheuvel, M. Z. Bazant, Phys. Rev. E 81 (2010) 031502.

[48] J. Lyklema, Fundamentals of Interface and Colloid Science, vol. II: Solid-Liquid Interfaces, Academic Press, New York, 1995.

[49] G. I. Guerrero-García, E. González-Tovar, M. Lozada-Cassou, F. D. Guevara-Rodríguez, J. Chem. Phys. 123 (2005) 034703.

[50] R. Messina, J. Phys.-Condens. Matt. 21 (2009) 113102.

[51] M. S. Kilic, M. Z. Bazant, A. Ajdari, Phys. Rev. E 75 (2007) 021502.

[52] P. M. Biesheuvel, M. van Soestbergen, J. Colloid Interface Sci. 316 (2007) 490–499.

[53] Z. Adamczyk, P. Warszynski, Adv. Colloid Interface Sci. 63 (1996) 41–149.

[54] I. Borukhov, J. Polymer Sci. Part B-Polymer Phys. 42 (2004) 3598–3615.

[55] J. Bockris, A. Reddy, Modern Electrochemistry, Plenum, New York, 1970.

[56] E. Wernersson, R. Kjellander, J. Lyklema, J. Phys. Chem. C 114 (2010) 1849–1866.

[57] M. Quesada-Perez, E. Gonzalez-Tovar, A. Martin-Molina, M. Lozada-Cassou, R. Hidalgo-lvarez, ChemPhysChem 4 (2003) 234–248.
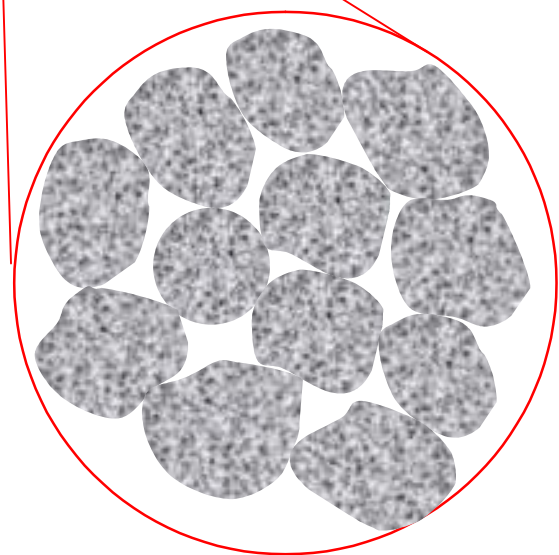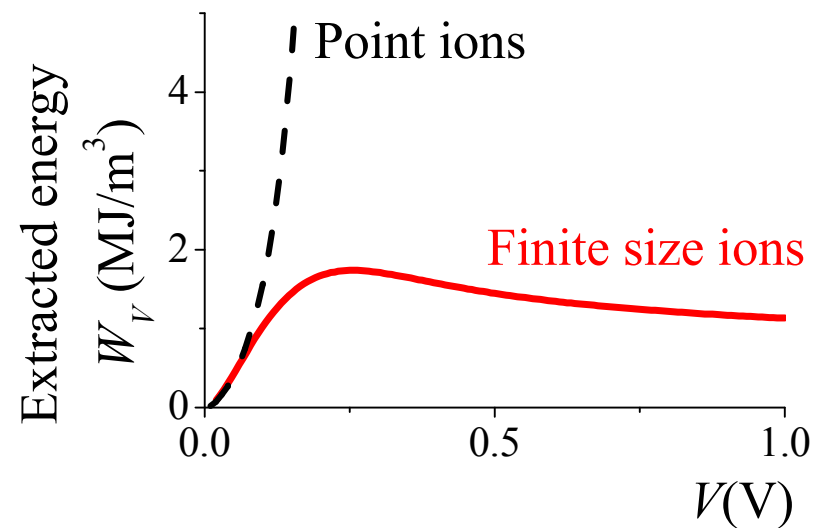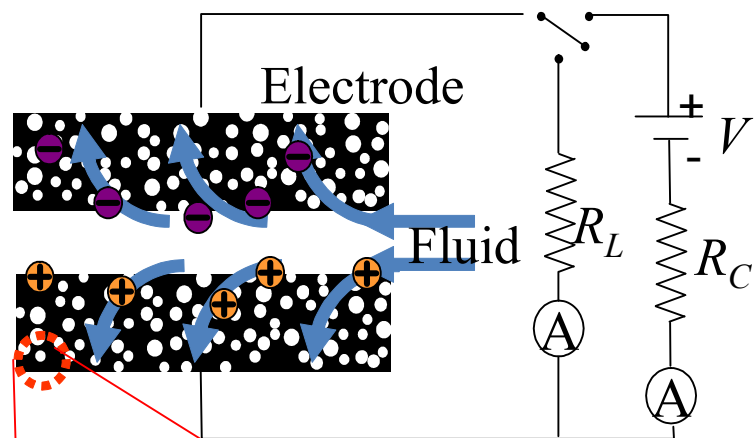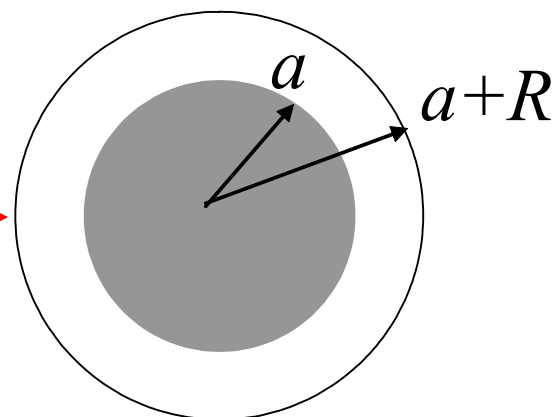
Predictions of the maximum energy extracted from salinity exchange inside porous electrodes

M.L. Jiménez, M.M. Fernández, S. Ahualli, G. Iglesias, A.V. Delgado

Highlights

- A study is presented of the electric double layer expansion in porous electrodes.

- The energy production associated to sea and fresh water exchange is discussed.

- The effect of finite ion size on the energy output is carefully considered.

- As a rule, modelling based on finite ion volumes predict lower work production.

- Significantly, a bell shape is found for the energy-wall potential relationship.

1